



**QUEEN'S
UNIVERSITY
BELFAST**

Multi-Way Massive MIMO with Maximum-Ratio Processing and Imperfect CSI

Chung, H. D., Ngo, H. Q., Matthaiou, M., & Duong, T. Q. (2017). Multi-Way Massive MIMO with Maximum-Ratio Processing and Imperfect CSI. In *25th European Signal Processing Conference (EUSIPCO): Proceedings* (Signal Processing Conference (EUSIPCO): Proceedings). Institute of Electrical and Electronics Engineers Inc.. <https://doi.org/10.23919/EUSIPCO.2017.8081500>

Published in:

25th European Signal Processing Conference (EUSIPCO): Proceedings

Document Version:

Peer reviewed version

Queen's University Belfast - Research Portal:

[Link to publication record in Queen's University Belfast Research Portal](#)

Publisher rights

© 2017 IEEE.

This work is made available online in accordance with the publisher's policies. Please refer to any applicable terms of use of the publisher.

General rights

Copyright for the publications made accessible via the Queen's University Belfast Research Portal is retained by the author(s) and / or other copyright owners and it is a condition of accessing these publications that users recognise and abide by the legal requirements associated with these rights.

Take down policy

The Research Portal is Queen's institutional repository that provides access to Queen's research output. Every effort has been made to ensure that content in the Research Portal does not infringe any person's rights, or applicable UK laws. If you discover content in the Research Portal that you believe breaches copyright or violates any law, please contact openaccess@qub.ac.uk.

Open Access

This research has been made openly available by Queen's academics and its Open Research team. We would love to hear how access to this research benefits you. – Share your feedback with us: <http://go.qub.ac.uk/oa-feedback>

Multi-Way Massive MIMO with Maximum-Ratio Processing and Imperfect CSI

Chung Duc Ho*, Hien Quoc Ngo*[†], Michail Matthaiou*, and Trung Q. Duong*

*Institute of Electronics, Communications and Information Technology (ECIT), Queens University Belfast, Belfast, BT3 9DT, U.K.

[†]Department of Electrical Engineering (ISY), Linköping University, 581 83 Linköping, Sweden

Email: {choduc01, m.matthaiou, trung.q.duong}@qub.ac.uk, hien.ngo@liu.se

Abstract—This paper considers a multi-way massive multiple-input multiple-output amplify-and-forward relaying system, where single-antenna users exchange their information-bearing signals with the assistance of one relay station equipped with unconventionally many antennas. The relay first estimates the channels to all users through the pilot signals transmitted from them. Then, the relay uses maximum-ratio processing (i.e. maximum-ratio combining in the multiple-access phase and maximum-ratio transmission in the broadcast phase) to process the signals. A rigorous closed-form expression for the spectral efficiency is derived. We show that by deploying massive antenna arrays at the relay and simple maximum-ratio processing, we can serve many users in the same time-frequency resource, while maintaining a given quality-of-service for each user.

Index Terms—Channel state information, massive MIMO, multi-way relay networks.

I. INTRODUCTION

In multi-way relay networks, many users simultaneously exchange their bearing information among them via the help of a single sharing relay at the same time-frequency resource [1]. Multi-way relay networks provide spatial diversity, and hence, they can scale up the spectral efficiency of the system without increasing the system complexity. In [2], the authors showed that the spectral efficiency of multi-way relay networks is much higher than that of one-way or two-way networks. Hence, these systems have been considered for diverse applications, such as wireless conference and power control in heterogeneous cellular networks, to name a few

Massive multiple-input multiple-output (MIMO), where a base station equipped with hundreds of antennas serves many active users in the same time-frequency resource, is considered as one of the key candidates for next-generation wireless systems [3], [4]. In [3], the authors showed that massive MIMO can substantially reduce the effects of noise, small-scale fading and inter-user interference by using simple linear processing, including maximum-ratio (MR) or/and zero-forcing (ZF) techniques. In particular, the transmit power of each user can be made inversely proportional to the number of antennas at the base station. Furthermore, the performance of the system can be scaled up noticeably without increasing the system complexity.

Multi-way massive MIMO relay networks, which combine massive MIMO and multi-way relaying technologies, have received research interest recently [5]. This is because they can leverage the benefits of both massive MIMO and multi-way relaying. Therefore, they are considered as a strong candidate to offer a noticeable improvement of spectral and energy efficiency [6], [7]. However, these works consider ZF processing at the relay which involves a complicated matrix inversion. Moreover, in massive MIMO, channel acquisition is a critical problem, and hence, the issue of imperfect channel state information should be taken into account.

Inspired by the above discussion, in this paper we consider a multi-way massive MIMO with MR processing and imperfect channel state information (CSI) under the amplify-and-forward (AF) protocol.

We note that when the number of antennas is large, ZF processing scheme is much more complicated than MR processing technique [8]. Most importantly, MR processing can be performed in a distributed fashion without large backhaul requirements. A complete transmission protocol under time-division duplex (TDD) operation is proposed. We derive a corresponding expression for the spectral efficiency in closed-form. Based on this closed-form expression, the effect of the number of relay antennas, imperfect channel estimation, and the number of users is analyzed.

Notations: The superscripts $(\cdot)^T$, $(\cdot)^*$, and $(\cdot)^H$ denote the transpose, conjugate, and Hermitian, respectively. The symbol $\|\cdot\|$ indicates the norm of a vector. The notations $\mathbb{E}\{\cdot\}$ and $\mathbb{V}\text{ar}\{\cdot\}$ are the expectation and the variance operators, respectively; $[\mathbf{X}]_{mn}$ or x_{mn} denotes the (m, n) -th entry of matrix \mathbf{X} , and \mathbf{I}_K is the $K \times K$ identity matrix. Moreover, $[\mathbf{X}]_k$ or \mathbf{x}_k denotes the k -th column of matrix \mathbf{X} .

II. SYSTEM MODEL

We consider a multi-way relaying massive MIMO system which consists of one relay equipped with M antennas, and K single-antenna users ($M \gg K$). The K users exchange information with each other with the help of the relay by sharing the same time-frequency resource. The k -th user wants to decode all $K - 1$ signals transmitted from other users. We make the assumption that all nodes operate in the half-duplex mode and the direct links (user-to-user links) do not exist due to the large obstacles and/or severe shadowing. Denote by \mathbf{G} the $M \times K$ channel matrix between the relay and the K users. In addition, \mathbf{G} models independent small-scale fading (Rayleigh fading) and large-scale fading (geometric attenuation and log-normal shadow fading). Also, we have that the channel coefficient between the m -th antenna of the relay and the k -th user is defined as

$$g_{mk} = h_{mk} \sqrt{\beta_k}, \quad (1)$$

where $h_{mk} \sim \mathcal{CN}(0, 1)$ represents the small-scale fading, and β_k represents the large-scale fading. In matrix form,

$$\mathbf{G} = \mathbf{H}\mathbf{D}^{1/2}, \quad (2)$$

where \mathbf{H} is an $M \times K$ matrix, $[\mathbf{H}]_{mk} = h_{mk}$ and \mathbf{D} is a $K \times K$ diagonal matrix, where $[\mathbf{D}]_{kk} = \beta_k$.

The transmission leverages TDD operation, and is divided into three phases: i) channel estimation; ii) multiple-access (MA); and iii) broadcast (BC) phases.

A. Channel Estimation Phase

The relay node needs to know the channel for performing digital signal processing. To do this, a part of coherence interval is used for channel estimation. For each coherence interval of length T symbols, all users simultaneously transmit pilot sequences of length τ symbols

to the relay. Let $\phi_k \in \mathbb{C}^{\tau \times 1}$ be the pilot sequence sent from the k -th user. We assume that $\phi_1, \phi_2, \dots, \phi_K$ are unit norm vectors and pairwise orthogonal, i.e., $\phi_k^H \phi_{k'} = 0$ for $k \neq k'$. This requires that $\tau \geq K$.

The $M \times \tau$ received pilot matrix at relay is given by

$$\mathbf{Y}_p = \sum_{k=1}^K \sqrt{\tau P_p} \mathbf{g}_k \phi_k^H + \mathbf{N}_p = \sqrt{\tau P_p} \mathbf{G} \Phi^H + \mathbf{N}_p, \quad (3)$$

where $\Phi \triangleq [\phi_1, \phi_2, \dots, \phi_K]$, P_p is the transmit power of each pilot symbol, \mathbf{g}_k is the k -th column of \mathbf{G} , and \mathbf{N}_p is the additive white Gaussian noise (AWGN) matrix with i.i.d. $\mathcal{CN}(0, 1)$ components.

At the relay, we apply the minimum mean-square-error (MMSE) technique to estimate the channel matrix \mathbf{G} [10]. The MMSE channel estimate of \mathbf{G} is

$$\hat{\mathbf{G}} = \frac{1}{\sqrt{\tau P_p}} \mathbf{Y}_p \Phi \tilde{\mathbf{D}} = \left(\mathbf{G} + \frac{1}{\sqrt{\tau P_p}} \tilde{\mathbf{N}}_p \right) \tilde{\mathbf{D}}, \quad (4)$$

where $\tilde{\mathbf{D}} \triangleq \left(\frac{\mathbf{D}^{-1}}{\tau P_p} + \mathbf{I}_K \right)^{-1}$ and $\tilde{\mathbf{N}}_p \triangleq \mathbf{N}_p \Phi$. From the property of Φ , the elements of $\tilde{\mathbf{N}}_p$ are i.i.d. $\mathcal{CN}(0, 1)$ random variables (RVs). Let \mathbf{E} be the estimation error matrix. Then,

$$\mathbf{G} = \hat{\mathbf{G}} + \mathbf{E}. \quad (5)$$

From the property of MMSE estimation, $\hat{\mathbf{G}}$ and \mathbf{E} are independent. We have $\hat{\mathbf{G}} \sim \mathcal{CN}(0, \hat{\mathbf{D}})$ and $\mathbf{E} \sim \mathcal{CN}(0, \mathbf{D}_E)$, where $\hat{\mathbf{D}}$ and \mathbf{D}_E are diagonal matrices with

$$[\mathbf{D}]_{kk} = \sigma_k^2 = \frac{\tau P_p \beta_k^2}{\tau P_p \beta_k + 1}, \quad \text{and} \quad [\mathbf{D}_E]_{kk} = \sigma_{e,k}^2 = \beta_k - \sigma_k^2. \quad (6)$$

B. Multiple-Access Phase

In this phase, data is transmitted to the relay in the same time-frequency resource from all users. The $M \times 1$ received vector at the relay is

$$\mathbf{y}_R = \sqrt{P_u} \mathbf{G} \mathbf{x} + \mathbf{n}, \quad (7)$$

where $\mathbf{x} = [x_1, \dots, x_K]^T$, with $\mathbb{E}\{|x_k|^2\} = 1$, is the $K \times 1$ signal vector transmitted from the K users, \mathbf{n} is an $M \times 1$ AWGN vector with i.i.d. $\mathcal{CN}(0, 1)$ components, and P_u is the transmit power of each user. Then, the relay uses the channel estimate in the channel estimation phase and employs the MR combining scheme as:

$$\tilde{\mathbf{y}}_R = \hat{\mathbf{G}}^H \mathbf{y}_R. \quad (8)$$

C. Broadcast Phase

In this phase, the relay spends $K - 1$ time-slots to transmit all signals to K users. The relay employs the MR scheme to broadcast a permuted version of $\tilde{\mathbf{y}}_R$ at each time-slot [6]. The transmit signal vector at the relay for the t -th ($t = 1, 2, \dots, K - 1$) time-slot can be expressed as

$$\mathbf{s}_R^{(t)} = \sqrt{\alpha^{(t)}} \hat{\mathbf{G}}^* \mathbf{\Pi}^{(t)} \tilde{\mathbf{y}}_R = \sqrt{P_u \alpha^{(t)}} \mathbf{A}^{(t)} \mathbf{x} + \sqrt{\alpha^{(t)}} \mathbf{B}^{(t)} \mathbf{n}, \quad (9)$$

where $\mathbf{\Pi}^{(t)} \in \mathbb{C}^{K \times K}$ is the permutation matrix for time slot t given as [6],

$$\mathbf{\Pi}^{(t)} = \begin{bmatrix} 0 & 1 & 0 & \dots & 0 & 0 \\ 0 & 0 & 1 & \dots & 0 & 0 \\ \vdots & \vdots & \vdots & \ddots & \vdots & \vdots \\ 0 & 0 & \dots & \dots & 1 & 0 \\ 0 & 0 & \dots & \dots & 0 & 1 \\ 1 & 0 & \dots & \dots & 0 & 0 \end{bmatrix}^t, \quad (10)$$

$\mathbf{A}^{(t)} = \hat{\mathbf{G}}^* \mathbf{\Pi}^{(t)} \hat{\mathbf{G}}^H \mathbf{G}$, $\mathbf{B}^{(t)} = \hat{\mathbf{G}}^* \mathbf{\Pi}^{(t)} \hat{\mathbf{G}}^H$. In (9), $\alpha^{(t)}$ is the normalization factor, chosen to satisfy a long-term power constraint at the relay,

$$\mathbb{E} \left\{ \left\| \mathbf{s}_R^{(t)} \right\|^2 \right\} = P. \quad (11)$$

From (7), (8), (9), and (11) the normalization factor $\alpha^{(t)}$ can be expressed as

$$\alpha^{(t)} = \frac{P_t}{P_u \sum_{k=1}^K \mathbb{E} \left\{ \left\| [\mathbf{A}^{(t)}]_k \right\|^2 \right\} + \sum_{m=1}^M \mathbb{E} \left\{ \left\| [\mathbf{B}^{(t)}]_m \right\|^2 \right\}}. \quad (12)$$

Then, the $K \times 1$ received signal vector at the K users in the t -th time slot can be described as follows:

$$\mathbf{y}_u^{(t)} = \mathbf{G}^T \mathbf{s}_R^{(t)} + \mathbf{w}^{(t)}, \quad (13)$$

and substituting (9) into (13), we obtain

$$\mathbf{y}_u^{(t)} = \sqrt{\alpha^{(t)} P_u} \mathbf{G}^T \mathbf{A}^{(t)} \mathbf{x} + \sqrt{\alpha^{(t)}} \mathbf{G}^T \mathbf{B}^{(t)} \mathbf{n} + \mathbf{w}^{(t)}. \quad (14)$$

III. SPECTRAL EFFICIENCY ANALYSIS

In this section, we analyse the spectral efficiency of the system. More specifically, we derive a closed-form expression for the spectral efficiency. Without loss of generality, we analyze the performance of the system in the first time-slot. The performance analysis for other time-slots follows the same methodology. Note that, hereafter, if $k = K$, then we set $k + 1 = 1$ and $k + 2 = 2$; if $k = 1$, then we set $k - 1 = K$; and if $k = 2$, we set $k - 2 = K$.

In the first time-slot, the k -th user wants to detect the signal x_{k+1} transmitted from the $(k + 1)$ -th user. From (14), the received signal in the first time slot for the k -th user is described by

$$\begin{aligned} y_{u,k}^{(1)} &= \sqrt{\alpha^{(1)} P_u} \mathbf{g}_k^T \mathbf{a}_{k+1}^{(1)} x_{k+1} + \sqrt{\alpha^{(1)} P_u} \sum_{\substack{i=1 \\ i \neq (k+1)}}^K \mathbf{g}_k^T \mathbf{a}_i^{(1)} x_i \\ &+ \sqrt{\alpha^{(1)}} \sum_{m=1}^M \mathbf{g}_k^T \mathbf{b}_m^{(1)} n_m + w_k^{(1)} \end{aligned} \quad (15)$$

$$= \underbrace{\sqrt{\alpha^{(1)} P_u} \mathbb{E} \left\{ \mathbf{g}_k^T \mathbf{a}_{k+1}^{(1)} \right\}}_{\text{desired signal}} x_{k+1} + \underbrace{\tilde{N}_k^{(1)}}_{\text{effective noise}}, \quad (16)$$

where $\tilde{N}_k^{(1)}$ is considered as the effective noise and given by

$$\begin{aligned} \tilde{N}_k^{(1)} &= \underbrace{\sqrt{\alpha^{(1)} P_u} \left(\mathbf{g}_k^T \mathbf{a}_{k+1}^{(1)} - \mathbb{E} \left\{ \mathbf{g}_k^T \mathbf{a}_{k+1}^{(1)} \right\} \right)}_{\text{beamforming uncertainty}} x_{k+1} \\ &+ \underbrace{\sqrt{P_u} \alpha^{(1)} \sum_{\substack{i=1 \\ i \neq (k+1)}}^K \mathbf{g}_k^T \mathbf{a}_i^{(1)} x_i}_{\text{inter-user interference}} + \underbrace{\sqrt{\alpha^{(1)}} \sum_{m=1}^M \mathbf{g}_k^T \mathbf{b}_m^{(1)} n_m + w_k^{(1)}}_{\text{noise}}. \end{aligned}$$

From (16), it can be clearly seen that the ‘‘desired signal’’ term is uncorrelated with the ‘‘effective noise’’ term. Therefore, the signal-to-interference-plus-noise ratio (SINR) for the k -th user in the first time-slot can be written as

$$\gamma_k^{(1)} = \frac{\alpha^{(1)} P_u \left| \mathbb{E} \left\{ \mathbf{g}_k^T \mathbf{a}_{k+1}^{(1)} \right\} \right|^2}{\alpha^{(1)} P_u \text{Var} \left(\mathbf{g}_k^T \mathbf{a}_{k+1}^{(1)} \right) + \text{IU}_k + \text{AN}_k + 1}, \quad (17)$$

$$\alpha^{(1)} = \frac{P_r}{M^3 P_u \sum_{k'=1}^K \sigma_{k'-1}^2 \sigma_{k'}^4 + M^2 \left(\sum_{k'=1}^K \sigma_{k'}^2 \sigma_{k'+1}^2 \right) \left(P_u \sum_{k'=1}^K \beta_{k'} + 1 \right) + M P_u \sum_{k'=1}^K \sigma_{k'}^4 \sigma_{k'+1}^2}, \quad (20)$$

where

$$\text{IU}_k = \alpha^{(1)} P_u \sum_{\substack{i=1 \\ i \neq (k+1)}}^K \mathbb{E} \left\{ \left| \mathbf{g}_k^T \mathbf{a}_i^{(1)} \right|^2 \right\}, \quad (18)$$

$$\text{AN}_k = \alpha^{(1)} \sum_{m=1}^M \mathbb{E} \left\{ \left| \mathbf{g}_k^T \mathbf{b}_m^{(1)} \right|^2 \right\}. \quad (19)$$

In (17), $\alpha^{(1)}$ is given by (12), and it can be represented in closed-form via (20) shown on the top of the page. The detailed derivation of (20) is shown in Appendix VI-A. Then, the spectral efficiency of the k -th user in bit/s/Hz is given by

$$\text{SE}_k^{(1)} = \left(\frac{T - \tau}{T} \right) \left(\frac{K - 1}{K} \right) \log_2 \left(1 + \gamma_k^{(1)} \right). \quad (21)$$

The pre-log factor in (21) includes: i) $\frac{T - \tau}{T}$ which comes from the fact that during a coherence interval of T symbols, we spend τ symbols for the training; and ii) $\frac{K - 1}{K}$ since we need K time slots to transfer $K - 1$ signals to a given user. We next provide a closed-form expression for the spectral efficiency given in (21).

Theorem 1: The closed-form expression for the spectral efficiency (21) is

$$\text{SE}_k^{(1)} = \left(\frac{T - \tau}{T} \right) \left(\frac{K - 1}{K} \right) \times \log_2 \left(1 + \frac{\alpha^{(1)} P_u M^4 \sigma_k^4 \sigma_{k+1}^4}{\alpha^{(1)} P_u \text{Var} \left\{ \mathbf{g}_k^T \mathbf{a}_{k+1}^{(1)} \right\} + \text{IU}_k + \text{AN}_k + 1} \right), \quad (22)$$

where

$$\text{Var} \left\{ \mathbf{g}_k^T \mathbf{a}_{k+1}^{(1)} \right\} = M^3 \mathbf{a}_{k,k+1} + M^2 \mathbf{b}_{k,k+1} + M \mathbf{c}_{k,k+1}, \quad (23)$$

$$\begin{aligned} \text{IU}_k &= \alpha^{(1)} P_u \sum_{\substack{i=1 \\ i \neq (k+1)}}^K (M^3 \mathbf{a}_{k,i} + M^2 \mathbf{b}_{k,i} + M \mathbf{c}_{k,i}) \\ &+ \alpha^{(1)} P_u M^2 \sigma_{k-1}^4 \sigma_k^4 + \alpha^{(1)} P_u M \left[2 \sigma_k^6 \sigma_{k+1}^2 + 2 \sigma_k^6 \sigma_{k-1}^2 \right. \\ &\left. + (2 \sigma_k^4 + \beta_k^2 - 2 \beta_k \sigma_k^2) \sum_{k'=1}^K 2 \sigma_{k'}^2 \sigma_{k'+1}^2 \right], \end{aligned} \quad (24)$$

$$\text{AN}_k = \alpha^{(1)} \left(M^3 \sigma_k^4 \sigma_{k+1}^2 + M^2 \beta_k \sum_{k'=1}^K \sigma_{k'}^2 \sigma_{k'+1}^2 \right), \quad (25)$$

where

$$\mathbf{a}_{k,i} = \sigma_k^4 \sigma_{k+1}^2 \beta_i + \sigma_i^4 \sigma_{i-1}^2 \beta_k, \quad (26)$$

$$\mathbf{b}_{k,i} = \beta_k \beta_i \sum_{k'=1}^K \sigma_{k'}^2 \sigma_{k'+1}^2, \quad (27)$$

$$\mathbf{c}_{k,i} = \sigma_k^4 \sigma_{k-1}^2 \beta_i + \sigma_i^4 \sigma_{i+1}^2 \beta_k. \quad (28)$$

Proof 1: See Appendix VI-B.

Result (22) yields some important remarks:

- As $M \rightarrow \infty$, the numerator of the SINR of (22) scales as M while the denominator converges to a constant, and hence, the spectral efficiency grows without bound.

- If the transmit power of each user is scaled with $1/M$, i.e. $P_u = E_u/M$, where E_u is fixed, then as $M \rightarrow \infty$, the spectral efficiency converges to

$$\text{SE}_k^{(1)} \rightarrow \left(\frac{T - \tau}{T} \right) \left(\frac{K - 1}{K} \right) \log_2 \left(1 + E_u \sigma_{k+1}^2 \right). \quad (29)$$

The result in (29) implies that by utilizing very large number of antennas M at the relay, the transmit power of each user can be scaled down proportionally to $1/M$ without reducing the system performance.

- If the transmit power at the relay is scaled with $1/M$, i.e., $P_r = E_r/M$, where E_r is fixed, then as $M \rightarrow \infty$, we obtain

$$\text{SE}_k^{(1)} \rightarrow \left(\frac{T - \tau}{T} \right) \left(\frac{K - 1}{K} \right) \log_2 \left(1 + \frac{E_r \sigma_k^4 \sigma_{k+1}^4}{\sum_{k'=1}^K \sigma_{k'}^2 \sigma_{k'+1}^2} \right), \quad (30)$$

which showcases that the transmit power at the relay can be reduced proportionally to $1/M$, for large M .

- If the transmit power of the relay and each user are scaled with $1/M$, i.e. $P_r = E_r/M$, and $P_u = E_u/M$, where E_r and E_u are fixed, then as $M \rightarrow \infty$, the spectral efficiency converges to

$$\text{SE}_k^{(1)} \rightarrow \left(\frac{T - \tau}{T} \right) \left(\frac{K - 1}{K} \right) \log_2 \left(1 + \frac{\xi E_u \sigma_k^4 \sigma_{k+1}^4}{\xi \sigma_k^4 \sigma_{k+1}^2 + 1} \right), \quad (31)$$

where

$$\xi = \frac{E_r}{\sum_{k'=1}^K (E_u \sigma_{k'-1}^2 \sigma_{k'}^4 + \sigma_{k'}^2 \sigma_{k'+1}^2)}. \quad (32)$$

We can see that, when M is large, the transmit power at the relay and each user can be cut down proportionally $1/M$, while maintaining a non-zero spectral efficiency.

IV. NUMERICAL RESULTS

In this section, numerical results are presented to verify our analysis. For all examples, we choose $T = 200$, and define SNR = P_u (expressed in dB). We examine the sum spectral efficiency as follows:

$$\text{SE}_{\text{sum}} = \sum_{k=1}^K \text{SE}_k^{(1)}. \quad (33)$$

We first consider a simple case where the large-scale fading $\beta_k = 1$ for all k . Figure 1 shows the sum spectral efficiency versus M for different K . The solid and circle lines present the Monte-Carlo simulations using (21) and analytical results using (22), respectively. From the figure, we can see that the analytical results match the simulation results which validates the correctness of our closed-form expression. As expected, when M increases the sum spectral efficiency increases. Furthermore, for low numbers of antennas, for example $M = 20$, the gaps of the sum spectral efficiency between the three cases ($K = 5, 10$, and 20) are very small. However, these gaps grow considerably when the number of antennas is large, i.e., at $M = 500$, the sum spectral efficiency with $K = 10$ is nearly double compared to the one with $K = 5$. This is due to the fact that when M increases, inter-user interference and noise effects are canceled out.

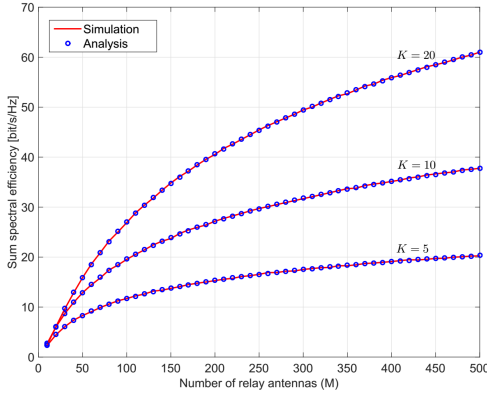


Fig. 1. Sum spectral efficiency against the number of relay antennas. We choose $T = 200$, $\tau = K$, $P_p = P_u = 0$ dB, $P_r = 10$ dB, and $\beta_k = 1$.

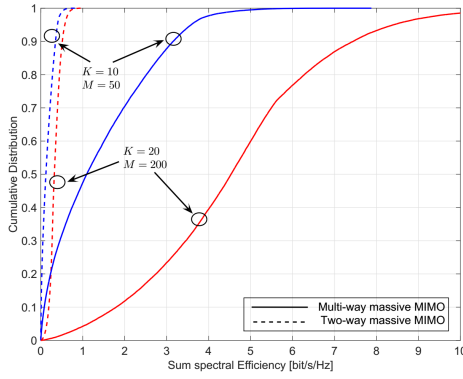


Fig. 2. Cumulative distribution of the sum spectral efficiency. We choose $D_d = 1000$ m, $T = 200$, $\tau = K$, $P_u = P_r = P_p = 0$ dB.

Next, we examine a more practical scenario that takes into account a realistic large-scale fading model. More precisely, the large-scale fading, is modeled by path loss and shadowing, given by [8]

$$\beta_k = \frac{z_k}{1 + \left(\frac{d_k}{d_0}\right)^\nu}, \quad (34)$$

where z_k is the log-normal random variable with standard deviations of σ_z dB, ν represents the path loss exponent, d_k is the distance between user k and the relay, and d_0 denotes a reference distance. Here, we assume that users are located uniformly at random inside a disk with a diameter D_d .

For our comparison, we also consider two-way massive MIMO relaying systems where the K users are grouped into $K(K-1)/2$ pairs, and each user is assigned different time-slots and uses the two-way relaying scheme to exchange data.¹ Since each pair requires two time-slots for information exchange, we need, in total, $K(K-1)$ time-slots to exchange all information among the K users. As a result,

¹Alternatively, one could consider a multi-pair two-way relaying protocol as in [11], where K sources exchange data with K destinations over two orthogonal time-slots (i.e., the number of users is always an even number). For this case, the pre-log factor is $1/2$. Compared with our multi-way relaying protocol, the multi-pair two-way relaying protocol has a smaller pre-log factor (when $K > 2$), but suffers a similar interference effect since multiple users transmit their data in the same time-frequency resource.

the spectral efficiency of the two-way massive MIMO relaying system is given by

$$\begin{aligned} \text{SE}_{\text{two-way},k}^{(1)} &= \left(\frac{T-\tau}{T}\right) \left(\frac{K-1}{K(K-1)}\right) \log_2(1 + \text{SINR}_k) \\ &= \left(\frac{T-\tau}{T}\right) \left(\frac{1}{K}\right) \log_2(1 + \text{SINR}_k), \end{aligned} \quad (35)$$

where SINR_k corresponds to the SINR in (22) for $K = 2$.

In this example, we choose $D_d = 1000$ m, $\sigma_z = 8$ dB, $\nu = 4$, $d_0 = 200$ m, $P_u = P_r = P_p = 0$ dB. Figure 2 demonstrates the cumulative distribution of the sum spectral efficiencies for two cases: $(K = 20, M = 200)$ and $(K = 10, M = 50)$. Compared to the two-way massive MIMO system, the multi-way massive MIMO system reduces the pre-log penalty (from $\frac{1}{K}$ to $\frac{K-1}{K}$), however, it exhibits more interference since many users simultaneously transmit data in the same frequency band. When M is large, the interference is small. Therefore, the multi-way massive MIMO system outperforms the two-way massive MIMO system, especially at large M .

V. CONCLUSION

We studied multi-way massive MIMO relay networks with MR processing and imperfect CSI. We derived a closed-form expression for the spectral efficiency. Our work showed that, by using a large antenna array at the relay, many users can simultaneously exchange their information in the same frequency band without any performance degradation for each user. As a result, multi-way massive MIMO offers much higher sum spectral efficiency than conventional multi-way MIMO or two-way massive MIMO systems do. Furthermore, as the number of relay antennas grows large, we can reduce the transmitted power at the relay and/or each user proportionally to $1/M$, while maintaining a given quality-of-service.

VI. APPENDICES

A. Derivation of (20)

The normalization factor $\alpha^{(1)}$ in (12) can be rewritten as

$$\alpha^{(1)} = \frac{P_r}{P_u \sum_{k=1}^K \mathbf{Q}_{1k} + P_u \sum_{k=1}^K \mathbf{Q}_{2k} + \sum_{m=1}^M \mathbf{Q}_{3m}}, \quad (36)$$

where

$$\mathbf{Q}_{1k} = \mathbb{E} \left\{ \left\| \left[\hat{\mathbf{G}}^* \mathbf{\Pi}^{(1)} \hat{\mathbf{G}}^H \hat{\mathbf{G}} \right]_k \right\|^2 \right\}, \quad (37)$$

$$\mathbf{Q}_{2k} = \mathbb{E} \left\{ \left\| \left[\hat{\mathbf{G}}^* \mathbf{\Pi}^{(1)} \hat{\mathbf{G}}^H \mathbf{E} \right]_k \right\|^2 \right\}, \quad (38)$$

$$\mathbf{Q}_{3m} = \mathbb{E} \left\{ \left\| \left[\hat{\mathbf{G}}^* \mathbf{\Pi}^{(1)} \hat{\mathbf{G}}^H \right]_m \right\|^2 \right\}. \quad (39)$$

First, we compute \mathbf{Q}_{1k} . We have,

$$\begin{aligned} \mathbf{Q}_{1k} &= \mathbb{E} \left\{ \left\| \left[\hat{\mathbf{G}}^* \mathbf{\Pi}^{(1)} \hat{\mathbf{G}}^H \hat{\mathbf{G}} \right]_k \right\|^2 \right\} \\ &= \mathbb{E} \left\{ \left\| \frac{\hat{\mathbf{g}}_{k+1}^H \hat{\mathbf{g}}_k}{\|\hat{\mathbf{g}}_k\|} \|\hat{\mathbf{g}}_k\| \|\hat{\mathbf{g}}_k^*\| \right\|^2 \right\} + \mathbb{E} \left\{ \|\hat{\mathbf{g}}_{k-1}^*\|^2 \|\hat{\mathbf{g}}_k\|^4 \right\} \\ &\quad + \sum_{\substack{k'=1 \\ k' \neq (k, k-1)}}^K \left\{ \left\| \hat{\mathbf{g}}_{k'}^* \hat{\mathbf{g}}_{k'+1}^H \hat{\mathbf{g}}_k \right\|^2 \right\} \\ &= \sigma_{k+1}^2 \mathbb{E} \left\{ \|\hat{\mathbf{g}}_k\|^4 \right\} + M \sigma_{k-1}^2 \mathbb{E} \left\{ \|\hat{\mathbf{g}}_k\|^4 \right\} \\ &\quad + \sum_{\substack{k'=1 \\ k' \neq (k, k-1)}}^K \left\{ \left\| \hat{\mathbf{g}}_{k'}^* \hat{\mathbf{g}}_{k'+1}^H \hat{\mathbf{g}}_k \right\|^2 \right\}, \end{aligned} \quad (40)$$

where in the last equality we have used the fact that $\frac{\hat{\mathbf{g}}_{k+1}^H \hat{\mathbf{g}}_k}{\|\hat{\mathbf{g}}_k\|} \sim \mathcal{CN}(0, \sigma_{k+1}^2)$ is independent of $\hat{\mathbf{g}}_k$ [3]. By using Lemma 2.9 in [9], (40) becomes

$$\begin{aligned} \mathbf{Q}_{1k} &= M(M+1)\sigma_k^4\sigma_{k+1}^4 + M^2(M+1)\sigma_{k-1}^2\sigma_k^4 \\ &+ M^2\sigma_k^2 \sum_{\substack{k'=1 \\ k' \neq (k, k-1)}}^K \sigma_{k'}^2\sigma_{k'+1}^2 \\ &= M^3\sigma_{k-1}^2\sigma_k^4 + M\sigma_k^4\sigma_{k+1}^2 + M^2\sigma_k^2 \sum_{k'=1}^K \sigma_{k'}^2\sigma_{k'+1}^2. \end{aligned} \quad (41)$$

Similarly, we obtain $\mathbf{Q}_{2k} = M^2(\beta_k - \sigma_k^2) \sum_{k'=1}^K \sigma_{k'}^2\sigma_{k'+1}^2$ and $\mathbf{Q}_{3m} = M \sum_{k'=1}^K \sigma_{k'}^2\sigma_{k'+1}^2$.

Substituting \mathbf{Q}_{1k} , \mathbf{Q}_{2k} and \mathbf{Q}_{3m} into (12), we obtain (20).

B. Proof of Theorem 1

1) Compute $\mathbb{E}\{\mathbf{g}_k^T \mathbf{a}_{k+1}^{(1)}\}$: Since $\hat{\mathbf{G}}$ and \mathbf{E} are independent. Then, we obtain

$$\begin{aligned} \mathbb{E}\{\mathbf{g}_k^T \mathbf{a}_{k+1}^{(1)}\} &= \mathbb{E}\left\{\mathbf{g}_k^T \left[\hat{\mathbf{G}}^* \mathbf{\Pi}^{(1)} \hat{\mathbf{G}}^H \hat{\mathbf{G}}\right]_{k+1}\right\} \\ &= \mathbb{E}\{\|\hat{\mathbf{g}}_k\|^2 \|\hat{\mathbf{g}}_{k+1}\|^2\} + \sum_{\substack{k'=1 \\ k' \neq k}}^K \mathbb{E}\left\{\hat{\mathbf{g}}_k^T \hat{\mathbf{g}}_{k'}^* \hat{\mathbf{g}}_{k'+1}^H \hat{\mathbf{g}}_{k+1}\right\} \\ &= M^2\sigma_k^2\sigma_{k+1}^2. \end{aligned} \quad (42)$$

2) Compute $\text{Var}\left(\mathbf{g}_k^T \mathbf{a}_{k+1}^{(1)}\right)$: From (42), the variance of $\mathbf{g}_k^T \mathbf{a}_{k+1}^{(1)}$ is given by

$$\begin{aligned} \text{Var}\left(\mathbf{g}_k^T \mathbf{a}_{k+1}^{(1)}\right) &= \mathbb{E}\left\{\left|\mathbf{g}_k^T \mathbf{a}_{k+1}^{(1)}\right|^2\right\} - \left|\mathbb{E}\left\{\mathbf{g}_k^T \mathbf{a}_{k+1}^{(1)}\right\}\right|^2 \\ &= \mathbb{E}\left\{\left|\mathbf{g}_k^T \mathbf{a}_{k+1}^{(1)}\right|^2\right\} - M^4\sigma_k^4\sigma_{k+1}^4 \\ &= \mathbb{E}\left\{\left|\left(\hat{\mathbf{g}}_k^T + \mathbf{e}_k^T\right) \hat{\mathbf{G}}^* \mathbf{\Pi}^{(1)} \hat{\mathbf{G}}^H \left(\hat{\mathbf{g}}_{k+1} + \mathbf{e}_{k+1}\right)\right|^2\right\} \\ &- M^4\sigma_k^4\sigma_{k+1}^4. \end{aligned} \quad (43)$$

Since $\hat{\mathbf{G}}$ and \mathbf{E} are independent, (43) can be rewritten as

$$\text{Var}\left(\mathbf{g}_k^T \mathbf{a}_{k+1}^{(1)}\right) = \mathbf{T}_1 + \mathbf{T}_2 + \mathbf{T}_3 + \mathbf{T}_4 - M^4\sigma_k^4\sigma_{k+1}^4, \quad (44)$$

where

$$\mathbf{T}_1 = \mathbb{E}\left\{\left|\hat{\mathbf{g}}_k^T \hat{\mathbf{G}}^* \mathbf{\Pi}^{(1)} \hat{\mathbf{G}}^H \hat{\mathbf{g}}_{k+1}\right|^2\right\}, \quad (45)$$

$$\mathbf{T}_2 = \mathbb{E}\left\{\left|\hat{\mathbf{g}}_k^T \hat{\mathbf{G}}^* \mathbf{\Pi}^{(1)} \hat{\mathbf{G}}^H \mathbf{e}_{k+1}\right|^2\right\}, \quad (46)$$

$$\mathbf{T}_3 = \mathbb{E}\left\{\left|\mathbf{e}_k^T \hat{\mathbf{G}}^* \mathbf{\Pi}^{(1)} \hat{\mathbf{G}}^H \hat{\mathbf{g}}_{k+1}\right|^2\right\}, \quad (47)$$

$$\mathbf{T}_4 = \mathbb{E}\left\{\left|\mathbf{e}_k^T \hat{\mathbf{G}}^* \mathbf{\Pi}^{(1)} \hat{\mathbf{G}}^H \mathbf{e}_{k+1}\right|^2\right\}. \quad (48)$$

To compute \mathbf{T}_1 , we rewrite (45) as

$$\begin{aligned} \mathbf{T}_1 &= \sum_{k'=1}^K \mathbb{E}\left\{\left|\hat{\mathbf{g}}_k^T \hat{\mathbf{g}}_{k'}^* \hat{\mathbf{g}}_{k'+1}^H \hat{\mathbf{g}}_{k+1}\right|^2\right\} \\ &= \mathbb{E}\{\|\hat{\mathbf{g}}_k\|^4\} \mathbb{E}\{\|\hat{\mathbf{g}}_{k+1}\|^4\} + \mathbb{E}\left\{\left|\hat{\mathbf{g}}_k^T \hat{\mathbf{g}}_{k+1}^* \hat{\mathbf{g}}_{k+2}^H \hat{\mathbf{g}}_{k+1}\right|^2\right\} \\ &+ \mathbb{E}\left\{\left|\hat{\mathbf{g}}_k^T \hat{\mathbf{g}}_{k-1}^* \hat{\mathbf{g}}_k^H \hat{\mathbf{g}}_{k+1}\right|^2\right\} + \sum_{\substack{k'=1 \\ k' \neq (k, k-1, k+1)}}^K \mathbb{E}\left\{\left|\hat{\mathbf{g}}_k^T \hat{\mathbf{g}}_{k'}^* \hat{\mathbf{g}}_{k'+1}^H \hat{\mathbf{g}}_{k+1}\right|^2\right\}. \end{aligned} \quad (49)$$

Again, by using Lemma 2.9 in [9], we get

$$\begin{aligned} \mathbf{T}_1 &= M^3(M+2)\sigma_k^4\sigma_{k+1}^4 + M\sigma_{k-1}^2\sigma_k^4\sigma_{k+1}^2 \\ &+ M\sigma_k^2\sigma_{k+1}^4\sigma_{k+2}^2 + M^2\sigma_k^2\sigma_{k+1}^2 \sum_{k'=1}^K \sigma_{k'}^2\sigma_{k'+1}^2. \end{aligned} \quad (50)$$

Similarly, we obtain

$$\begin{aligned} \mathbf{T}_2 &= M^3\sigma_{e, k+1}^2\sigma_k^4\sigma_{k+1}^2 + M\sigma_{e, k+1}^2\sigma_{k-1}^2\sigma_k^4 \\ &+ M^2\sigma_k^2\sigma_{e, k+1}^2 \sum_{k'=1}^K \sigma_{k'}^2\sigma_{k'+1}^2, \end{aligned} \quad (51)$$

$$\begin{aligned} \mathbf{T}_3 &= M^3\sigma_{e, k}^2\sigma_k^2\sigma_{k+1}^4 + M\sigma_{e, k}^2\sigma_{k+1}^4\sigma_{k+2}^2 \\ &+ M^2\sigma_{e, k}^2\sigma_{k+1}^2 \sum_{k'=1}^K \sigma_{k'}^2\sigma_{k'+1}^2, \end{aligned} \quad (52)$$

$$\mathbf{T}_4 = M^2\sigma_{e, k}^2\sigma_{e, k+1}^2 \sum_{k'=1}^K \sigma_{k'}^2\sigma_{k'+1}^2. \quad (53)$$

By using (6), and substituting (50), (51), (52) and (53) into (43), we arrive at the desired result as in (23).

3) Compute $\mathbf{I}\mathbf{U}_k$ and $\mathbf{A}\mathbf{N}_k$:

Following a similar methodological approach as in 1) and 2), we obtain $\mathbf{I}\mathbf{U}_k$ and $\mathbf{A}\mathbf{N}_k$ given in (24) and (25), respectively.

ACKNOWLEDGMENT

This work was supported by project no. 3811/QD-UBND, Binh Duong government, Vietnam. The work of H. Q. Ngo was supported by the Swedish Research Council (VR) and ELLIIT. The work of M. Matthaiou was supported in part by the EPSRC under grant EP/P000673/1. The work of T. Q. Duong was supported in part by the U.K. Royal Academy of Engineering Research Fellowship under Grant RF1415\14\22 and by the U.K. EPSRC under Grant EP/P019374/1.

REFERENCES

- [1] D. Gündüz, A. Yener, A. Goldsmith, and H. V. Poor, "The multiway relay channel," *IEEE Trans. Inf. Theory*, vol. 59, no. 1, pp. 51-63, Jan. 2013.
- [2] A. Amah and A. Klein, "Non-regenerative multi-way relaying with linear beamforming," in *Proc. IEEE PIMRC*, Sept. 2009, pp. 1843-1847.
- [3] H. Q. Ngo, E. G. Larsson, and T. L. Marzetta, "Energy and spectral efficiency of very large multiuser MIMO systems," *IEEE Trans. Commun.*, vol. 61, no. 4, pp. 1436-1449, Apr. 2013.
- [4] E. G. Larsson, O. Edfors, F. Tufvesson, T. L. Marzetta, "Massive MIMO for next generation wireless systems," *IEEE Commun. Mag.*, vol. 52, no. 2, pp. 186-195, Feb. 2014.
- [5] G. Amarasuriya, E. G. Larsson, and H. V. Poor, "Wireless information and power transfer in multi-way massive MIMO relay networks," *IEEE Trans. Wireless Commun.*, vol. 15, no. 6, pp. 3837-3855, June 2015.
- [6] G. Amarasuriya, C. Tellambura, and M. Ardakani, "Multi-way MIMO amplify-and-forward relay networks with zero-forcing transmission," *IEEE Trans. Commun.*, vol. 61, no. 12, pp. 847-863, Dec. 2013.
- [7] C. D. Ho, H. Q. Ngo, M. Matthaiou, and T. Q. Duong, "On the performance of zero-forcing processing in multi-way massive MIMO relay networks," *in press IEEE Commun. Lett.*
- [8] H. Q. Ngo, H. A. Suraweera, M. Matthaiou, and E. G. Larsson, "Multipair full-duplex relaying with massive arrays and linear processing," *IEEE J. Sel. Areas Commun.*, vol. 32, no. 9, pp. 1721-1737, Sept. 2014.
- [9] A. M. Tulino and S. Verdú, "Random matrix theory and wireless communication," *Foundations and Trends in Communications and Information Theory*, vol. 1, no. 1, pp. 1-182, Jun. 2004.
- [10] S. M. Kay, *Fundamentals of Statistical Signal Processing: Estimation Theory*. Englewood Cliffs, NJ: Prentice Hall, 1993.
- [11] C. Kong, C. Zhong, M. Matthaiou, E. Björnson, and Z. Zhang, "Multipair two-way half-duplex relaying with massive arrays and imperfect CSI," *IEEE Trans. Inf. Theory*, Jul. 2016, submitted. [Online]. Available: <https://arxiv.org/abs/1607.01598>.